

NOTES AND CORRESPONDENCE

An Upper Bound on the Size of Sub-mesoscale Coherent Vortices

LUANNE THOMPSON

*MIT-WHOI Joint Program in Physical Oceanography, MIT Center for Meteorology
and Physical Oceanography, Cambridge, Massachusetts*

W. R. YOUNG*

Department of Earth, Atmospheric and Planetary Sciences, Massachusetts Institute of Technology, Cambridge, Massachusetts

26 November 1987 and 27 April 1988

ABSTRACT

Laboratory experiments show that ageostrophic instability can "break up" a parallel flow into a sequence of axisymmetric eddies. This is a plausible scenario for the generation of sub-mesoscale coherent vortices (SCVs). Here we show that conservation of mass, energy and potential vorticity enables one to very simply calculate the radius of the axisymmetric eddy and the wavelength of the nonlinear instability. The latter agrees more closely with laboratory experiments than does the wavelength predicted by linearized stability theory. If energy is not conserved, say because of wave radiation into the lower layer, then the preceding calculation establishes an upper bound on the radius of the eddy. We offer this as an explanation of the observed small size of SCVs.

1. Introduction

Sub-mesoscale coherent vortices (SCVs) are recently discovered structures with properties distinct from those of mesoscale eddies. McWilliams (1985) reviews observations of SCVs. A complete discussion of a SCV investigated during the Local Dynamics Experiment is given in Riser et al. (1986). The important characteristics of SCVs for this paper follow. They have scales not exceeding the first baroclinic radius of deformation. They are usually anticyclonic, and their vertical structure is more localized than that of mesoscale eddies. They are very closely axisymmetric. Distinct water properties are carried by the SCVs, and by tracing these back to the source region, lifetimes of years have been inferred.

There are various models of isolated vortices that have been applied to SCVs. A review of these is given by McWilliams (1985); two examples are a one and one-half layer propagating β -plane monopole discussed by Nof (1981) and Killworth (1983), and a one and one-half layer f -plane monopole discussed by Flierl (1979) and Csanady (1979). These models have vanishing depth on the perimeter of the eddy and so are not quasi-geostrophic.

These solutions generally have a free parameter which is the mass or radius of the eddy. Thus, theoretically, there is no reason why arbitrarily large lenses

can not exist. Further, stability considerations restrict the aspect ratio of the eddy but do not imply selection of a particular size (McWilliams et al., 1986). It is then surprising that observations show an upper limit on the size of SCVs; they are not larger than the first baroclinic radius of deformation and are often smaller. It is this observation that we attempt to explain in this note. Our hypothesis, which is developed below, is that the various mechanisms that produce SCVs are subject to an energetic constraint which sharply limits the upper size of an axisymmetric structure produced by either disruptive instability of a parallel flow or penetrative convection driven by diapycnal mixing.

The generation of SCVs is not well understood and our arguments hinge on rather general considerations of mass and energy conservation. Before discussing these generalities, it is helpful to have a specific scenario in mind. McWilliams (1985) suggests a conceptual model for the generation of SCVs by mixing and adjustment. In this model, a diapycnal mixing process occurs. This mixing could be due to gravitational stirring, as in the case of a surface layer which is convectively unstable, or alternatively instability, which progresses to mixing as in inertial instability. The end state is a patch of water that is neutrally buoyant and is less stratified than its surroundings. The eddy then adjusts geostrophically to produce an anticyclonic circulation. A simplified version of the instability formation mechanism is the ageostrophic instability of a gravity current with two density fronts, which is treated analytically and experimentally by Griffiths et al. (1982, GKS hereafter).

Generally speaking, there are two types of nonlinear instability. First, an instability can equilibrate as a weakly nonlinear perturbation on the initial state. Finite amplitude perturbation theory does well in de-

* Present affiliation: Scripps Institution of Oceanography, La Jolla, CA.

Corresponding author address: Lu Anne Thompson, Dept. of Earth, Atmospheric and Planetary Sciences, Massachusetts Institute of Technology, Room 54-1419, Cambridge, MA 02139.

scribing the final state. More relevant to the present work, and GKS, is the second possibility in which an instability totally disrupts the initial configuration. This phenomenon is seen in the laboratory experiments of GKS. The parallel flow breaks up into a chain of axisymmetric eddies. Each of these subsequently evolves as a coherent structure and the relevance of their results to the generation of SCVs is clear.

In this paper, we discuss some constraints on the strongly nonlinear evolution of a disruptive instability, such as that which fragments a parallel flow into a chain of axisymmetric eddies. Conservation of energy, mass, and potential vorticity predicts the size of the axisymmetric vortex which is produced by the disruptive instability of a parallel flow.

The axisymmetric eddy is a one layer monopole with uniform potential vorticity (Flierl 1979; Csanady 1979). For simplicity we first consider the case where the potential vorticity is zero. In this instance there is an analytic solution which shows how the conservation of energy, E , and mass, M , implies a relation between the length of current to be broken, λ , the width of the current, $2L$, and the radius of the eddy, R . These lengths are illustrated in Fig. 1.

Using the shallow water equations the gravity current is geostrophically balanced

$$fu = -g'h_y$$

and has zero potential vorticity

$$q = u_y - f = 0.$$

Together with the boundary condition $h(\pm L) = 0$ these imply

$$u = fy$$

$$h = f^2(L^2 - y^2)/2g'.$$

Now one can calculate the energy and mass in a segment of length λ

$$E = (1/2)\lambda \int_{-L}^L hu^2 + g'h^2 dy = L^5 f^4 \lambda / 5g' \quad (1.1)$$

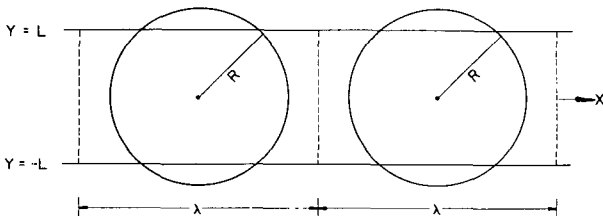


FIG. 1. Model geometry, showing the length of the parallel current λ that is broken off to form an axisymmetric eddy of radius R . The parallel flow is flowing in the x direction and has width $2L$. Note that in this process a series of eddies are formed.

$$M = \lambda \int_{-L}^L h dy = 2L^3 f^2 \lambda / 3g'. \quad (1.2)$$

For an axisymmetric eddy the azimuthal velocity is in cyclostrophic balance

$$fv + r^{-1}v^2 = g'h_r$$

and the potential vorticity is zero

$$v_r + r^{-1}v + f = 0.$$

We require $v(0) = 0$ and $h(R) = 0$ so that

$$v = -fr/2,$$

$$h = f^2(R^2 - r^2)/8g',$$

and then

$$E = \pi \int_0^R (hv^2 + g'h^2)r dr = \pi R^6 f^4 / 192g', \quad (1.3)$$

$$M = 2\pi \int_0^R hr dr = \pi R^4 f^2 / 16g'. \quad (1.4)$$

Now we can eliminate λ between (1.1) and (1.2) to obtain a connection between E and M for a parallel flow

$$E = 3f^2 L^2 M / 10. \quad (1.5)$$

Likewise R can be eliminated between (1.3) and (1.4) so that for an axisymmetric eddy, E and M are connected by

$$E = fg'^{1/2} M^{3/2} / \pi^{1/2} 3. \quad (1.6)$$

In comparing (1.5) and (1.6) we note that for a parallel flow the energy contained in a segment of length λ is just proportional to the volume in the same segment. However for an axisymmetric eddy the energy depends nonlinearly on the volume. We plot these two relations in Fig. 2. The point where the two curves intersect then gives λ , R , M and E in terms of L . Specifically

$$R = (18/5)^{1/2} L = 1.90L \quad (1.7)$$

$$\lambda = (243\pi/200)L = 3.82L.$$

A similar calculation is done in section 2 for other, nonzero, values of potential vorticity. In that section we also discuss the effects of dissipation. Because of the nonlinearity in the cyclostrophic balance this must be numerical, but the essential idea is identical to the preceding. There is, however, one other case in which some analytic progress is possible and this is the limit complementary to the above, when the uniform potential vorticity is large. More precisely when the non-dimensional potential vorticity

$$\hat{q} \equiv fL^2 q / g' \quad (1.8)$$

is much greater than one both the parallel flow and the axisymmetric eddy have an identical exponential boundary layer structure near the front. In this case

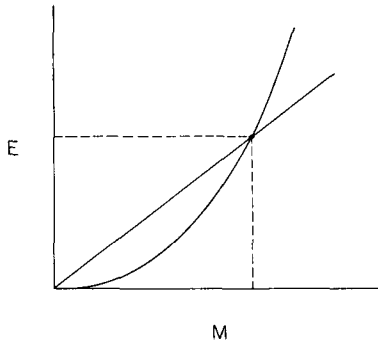


FIG. 2. Energy E versus mass M for a piece of parallel current of width $2L$ (straight line) and for an axisymmetric eddy. Both have zero potential vorticity. When the two curves intersect, the two systems have the same mass and energy. This point gives the relationships among R , L and λ as described in the text.

conservation of mass is equivalent to conservation of area

$$2L\lambda = \pi R^2,$$

and conservation of energy is equivalent to conserving the length of the front

$$2\lambda = 2\pi R.$$

Solving the above gives

$$R = 2L \tag{1.9}$$

$$\lambda = 2\pi L,$$

and comparing (1.7) to (1.9) the insensitivity of R to \hat{q} is noteworthy.

The preceding discussion shows that a vortex produced by the disruptive instability of a buoyancy current should have a particular scale selected as in Fig. 2. In principle a similar argument applies to vortices produced by penetrative convection. Suppose dense

water is produced at the sea surface and then falls to a neutrally buoyant level where it produces an axisymmetric eddy. As mass is added to the eddy its energy grows nonlinearly, e.g. (1.6). The source of energy is release of gravitational potential energy, but ultimately, because $dE/dM \propto M^{1/2}$, the addition of an extra bit of mass requires more energy than is released by the descent of the fluid from the surface. Thus a steady source of dense fluid at the surface plausibly produces a sequence of axisymmetric vortices of a particular size, rather than an ever expanding, single vortex. The point which is common to both this argument, and that leading to (1.7), is that an axisymmetric vortex has a nonlinear relation between its mass and energy whereas in the source these invariants are linearly proportional to each other. In this article we focus on vortex formation by the disruptive instability of a buoyancy current principally because this process is well documented in the literature and our results can be compared with experiments and numerical simulations.

2. Fragmentation of a constant potential vorticity buoyancy current

a. Numerical results

The structure of a uniform potential vorticity parallel flow can be found analytically, but for axisymmetric flow the nonlinear cyclostrophic terms necessitate numerical solution. In Fig. 3 the results of this calculation are summarized.

b. Comparison with laboratory results

To compare with the GKS experiments we must introduce some new notation. To nondimensionalize λ they used

$$L_r \equiv L[1 - \text{sech}(\hat{q}^{1/2})]^{1/2} \hat{q}^{-1/2} \tag{2.1}$$

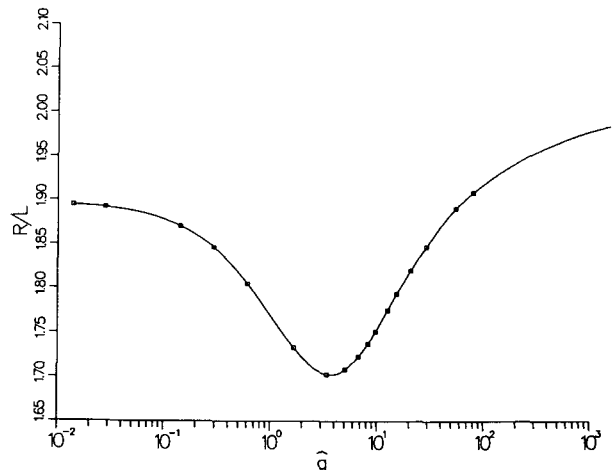
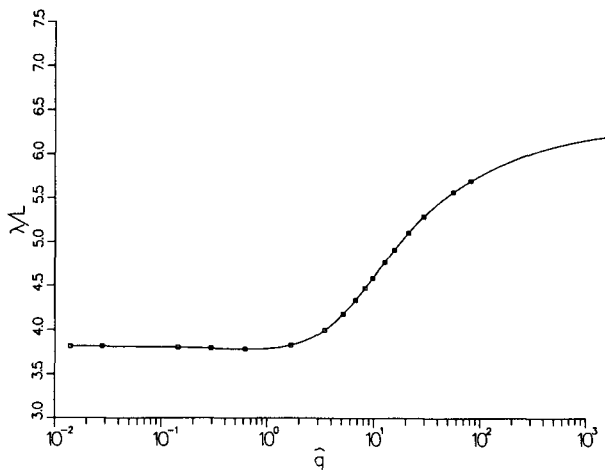


FIG. 3. (a) The length of the current λ broken off to form the eddy (nondimensionalized by L), the half width of the current versus \hat{q} as defined in (1.8). (b) The radius of the eddy nondimensionalized by L versus \hat{q} .

where \hat{q} is defined in (1.8). Here L_r is deformation radius based on the central depth of the buoyancy current.

Rather than using \hat{q} as an independent variable, GKS used the more easily measured parameter

$$L_0 = \hat{q}^{1/2} - \tanh \hat{q}^{1/2}. \quad (2.2)$$

The cross-sectional area of the buoyancy current is

$$A = \int_{-L}^L h dy. \quad (2.3)$$

In Fig. 4 L_r is used to nondimensionalize λ and L_0 , rather than \hat{q} , is used as a dimensionless variable. The results are plotted this way to be able to compare them easily with the results of GKS. From Fig. 4 we notice that the relevant parameter range when comparing our results to the laboratory experiments is $\hat{q} = O(1)$. Neither of the limiting cases $\hat{q} \rightarrow 0$ or $\hat{q} \rightarrow \infty$ is relevant to the laboratory experiments. In particular, for large values of \hat{q} the agreement with the laboratory experiment is not good. However, when \hat{q} is large ($L_0 > 2$, $q > 9$), GKS find a different type of instability in the laboratory experiment. The end state is no longer a chain of eddies, and our analysis would be expected to fail. In this limit GKS suggest that the second layer becomes important. If this is the case, some of the initial energy must go into the lower layer and the preceding calculation would have to be modified. For moderate values of \hat{q} however, the preceding model does sig-

nificantly better than linear stability theory at estimating λ .

c. Energy loss to molecular absorption contrasted with wave radiation into an active lower layer

During the collapse of the buoyancy current, there may be loss of energy due to the radiation of waves on the interface resulting in a transfer of energy to the lower layer. As in the Rossby adjustment problem (Gill 1982), potential vorticity of the upper layer is conserved, but energy is lost because of this radiation. To explore how this effect can change the size of the eddies, we once again consider the simple case of zero potential vorticity. The mass of the upper layer fluid is conserved, but the initial energy, E_i , contained in the parallel flow is larger than the final energy, E_f , contained in the axisymmetric eddy, i.e.

$$a \equiv E_i/E_f \quad (2.4)$$

where the parameter a is greater than one. Using (1.1)–(1.4) and (2.4) we find

$$R/L = (18/5a)^{1/2}$$

$$\lambda/L = 243\pi/200a^2.$$

We also performed numerical calculations for intermediate values at \hat{q} , that showed the same tendency to reduce the size of the eddies. Thus, if energy is lost to

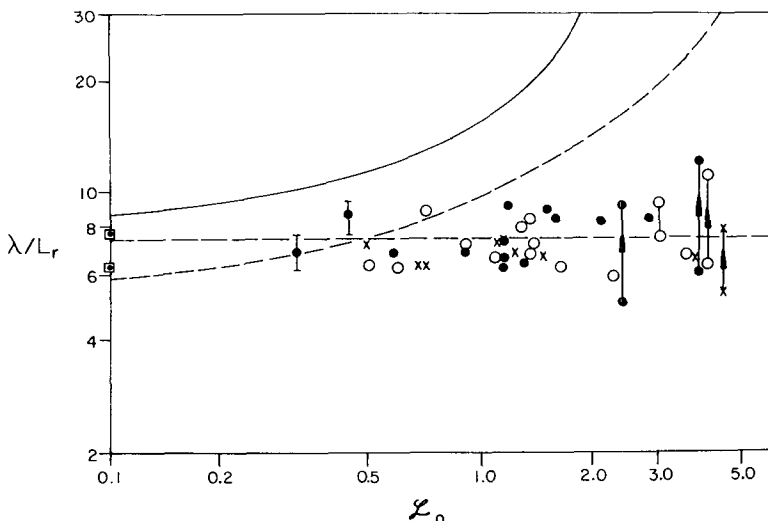


FIG. 4. The length of the parallel current λ [nondimensionalized by the Rossby radius of deformation given in (2.1) versus L_0 defined in (2.2)]. The dotted line is our result. The solid line is the result from the linear stability analysis of GKS where λ is the wavelength of the most unstable mode. The unconnected dots are results from the laboratory experiments of GKS, where λ is the circumference of the annulus divided by the number of eddies observed. The two square points are from a numerical model by Salmon (1983). The two different points come from two runs with different resolution and unfortunately the one that is further from our result has the higher resolution. However Salmon remarks that in this experiment the number of fluid particles per sampling are a is less than the other.

an active lower layer, the calculation presented gives an upper bound on the size of the eddies.

In the laboratory experiments done by GKS, when $\hat{q} > 9$, $L_0 > 2$, there is an active lower layer. In Fig. 4, our calculation overestimates the size of the eddies. When $\hat{q} = 9$, a loss of energy of 7% ($a = 1.07$) will bring the results into agreement with those of the laboratory. This indicates that only a small amount of energy is lost during the transition from parallel flow to axisymmetric flow.

Energy loss in this experiment from gravity wave radiation is much less than such loss in a Rossby adjustment problem. Perhaps this is because the break up is a transition from one adjusted state to another. In the experiment the transition occurs in six revolutions, slower than f^{-1} , and so little energy goes into gravity wave radiation.

Other dissipative processes, such as molecular viscosity, can change the energy and the potential vorticity of the fluid. This can lead to the production of larger eddies. To understand this, one need only note friction spreads a density intrusion laterally (Gill 1981). Thus if mass is added very slowly to an axisymmetric eddy then friction can result in a continuously expanding eddy.

Finally one might wonder if the instability observed by GKS relies in some essential way on dissipation or energy loss. If this were the case, the arguments given in this article would lose much of their force. However, Salmon's successful numerical simulation of the GKS instability, using a code that ensures conservation of both potential vorticity and energy, shows that dissipation is not required to fragment the gravity current. The instability is essential inviscid.

3. Conclusion

We show that if a gravity current with constant potential vorticity, bounded by two free streamlines, breaks up into a stream of axisymmetric eddies, con-

serving potential vorticity, energy, and mass, the radius of the eddies can be predicted. The length of the current that breaks off can also be related to the width of the current. This calculation is intended as a specific illustration of a more general idea which may have applicability to a broad range of problems. This is that the nonlinear relation between eddy energy and eddy mass can be used to constrain to possible outcome of a disruptive instability. For simplicity this initial investigation has used a one layer model but it is clear that similar constraints apply to more realistic multilayer models.

Acknowledgments. This research was supported by the Office of Naval Research Grant N00014-86-K-0325. WRY thanks Kerry Emanuel and Melvin Stern for interesting conversations during the early part of this work.

REFERENCES

- Csanady, C., 1979: The birth and death of a warm core ring. *J. Geophys. Res.*, **84**, 777-780.
- Flierl, G. R., 1979: A simple model for the structure of warm and cold core rings. *J. Geophys. Res.*, **84**, 781-785.
- Gill, A. E., 1982: *Atmosphere-Ocean Dynamics*, Academic Press, 662 pp.
- , 1981: Homogeneous intrusions in a rotating stratified fluid. *J. Fluid Mech.*, **103**, 275-295.
- Griffiths, R., P. Killworth and M. Stern, 1982: Ageostrophic instability of ocean currents. *J. Fluid Mech.*, **117**, 343-377.
- Killworth, P. D., 1983: On the motion of isolated lenses on a beta-plane. *J. Phys. Oceanogr.*, **13**, 368-376.
- McWilliams, J. C., 1985: Submesoscale, coherent vortices in the ocean. *Rev. Geophys.*, **23**, 165-182.
- , P. R. Gent and N. J. Norton, 1986: The evolution of balanced, low-mode vortices on the β -plane. *J. Phys. Oceanogr.*, **16**, 838-855.
- Nof, D., 1981, On the β -induced movement of isolated baroclinic eddies. *J. Phys. Oceanogr.*, **11**, 1662-1672.
- Riser, S. C., W. B. Owens, H. T. Rossby and C. C. Ebbesmeyer, 1986: The structure, dynamics, and origin of a small scale lens of water in the western North Atlantic thermocline. *J. Phys. Oceanogr.*, **16**, 572-590.
- Salmon, R., 1983: Practical uses of Hamilton's principle. *J. Fluid Mech.*, **132**, 431-444.